

## A Study on the Iodine-induced Stress Corrosion Cracking of Zircaloy-4 Cladding (I)

W.S. Ryu, S.I. Hong, Y. Choi, Y.H. Kang, C.S. Rim

Korea Advanced Energy Research Institute

(Received May 13, 1985)

지르칼로이-4 피복재의 요드응력 부식 균열에 대한 연구

류우석 · 홍순익 · 최 용 · 강영환 · 임창생

한국에너지연구소

(1985. 5. 13 접수)

### Abstract

Iodine-induced stress corrosion cracking tests of Zircaloy-4 cladding were undertaken using the modified internal pressurization method. The effects of iodine concentration and applied stress were studied. The critical iodine concentration for SCC was found to be about  $0.2 \text{ mg/cm}^2$  at  $603^\circ\text{K}$ . The threshold stress was dependent on the test temperature and the mechanical properties of the specimen. The fracture surface showed that the crack propagated stepwise from one grain to others until the material was unstable and then ruptured mechanically. The initial region showed the transgranular feature and the wedge-shaped cracks. As the crack proceeded, the transgranular and ductile-tearing mixed feature appeared in the middle region.

### 요 약

지르칼로이-4 피복재의 요드에 의한 응력부식 균열 현상을 개량된 내부가압방법으로 조사하였다. 요드 응력부식 균열 현상을 일으키는 임계요드농도와 임계 응력이 존재하였으며,  $603^\circ\text{K}$ 의 시험 온도에서 임계요드 농도는 약  $0.2 \text{ mg/cm}^2$ 였고 임계 응력은 시험온도와 시편의 기계적 성질에 따라 변하였다. 파괴면을 주사전자 현미경으로 관찰한 결과, 초기 단계는 입내 파손 형태로 W-형의 균열을 포함하고 있었으며, 균열이 진행됨에 따라 입내 파손과 연성 파손이 혼합된 형태로 나타남을 알 수 있었다. 그리고 균열은 한 결정립에서 다른 결정립으로 단계적으로 전파되어 나갔다.

### 1. Introduction

Iodine-induced stress corrosion cracking (I-SCC) of Zircaloy has been extensively studied in nuclear material laboratories,<sup>1-4)</sup> because iodine has been suggested one of the primary suspects of the chemical substance involved in

PCI (pellet cladding interaction). I-SCC behaviors of Zircaloy were dependent on test conditions such as stress, iodine concentration, test temperature and mechanical properties of Zircaloy, etc.<sup>5,6)</sup> There were the threshold value of stress under which I-SCC did not occur and the critical iodine concentration above which I-SCC occurred severely.<sup>7,8)</sup>

Some efforts have also included fractographic analysis of the fracture surface caused by I-SCC.<sup>9-11)</sup> It was noted that intergranular fracture took place during the initiation stage of I-SCC, while transgranular fracture was produced during the propagation stage. Recently, however, it was reported that only transgranular fracture was observed.<sup>10)</sup> In fact, once the fracture surface was damaged by oxidation, it was difficult to recognize the subtle difference between intergranular and transgranular feature.

There were many methods of laboratory I-SCC test that have been used in the various studies.<sup>2)</sup> Slotted ring test or mandrel test was one of the constant strain tests but could not avoid the effect of stress relaxation. Conventional internal pressurization test with reservoir was one of the constant stress tests and was not affected by stress relaxation but might not fix the iodine concentration in the specimen because iodine would diffuse out to the cold reservoir.

In this study, we used the modified internal pressurization method to fix the iodine concentration and avoid the oxidation of the fracture surface. The general I-SCC behaviors of Zircaloy, i.e. the effects of iodine concentration and stress, were studied. Fracture surface was observed using SEM to elucidate the I-SCC mechanism.

## 2. Experiment

The specimen used in the study was the commercially produced, stress-relieved Zircaloy-4 fuel cladding with 15 cm length. The test apparatus was shown in figs. 1 and 2. The specimen was connected to the pressurization system via stainless steel Swagelok fittings and pressurized with argon gas using the gas booster after evacuated at room temperature. The specimen internal pressure was measured by a pressure transducer. When the pressure reached the

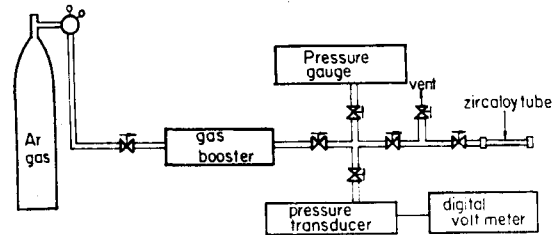


Fig. 1. Schematic Diagram of the Specimen Pressurization System.

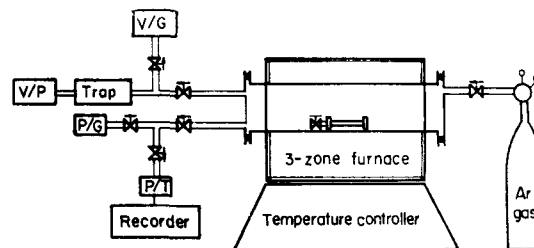


Fig. 2. Schematic Diagram of the Temperature Control and Time-to-failure Measurement System.

required value, the specimen was sealed and then isolated from the system. The isolated specimen was held in the chamber of an electric resistant 3-zone furnace with the  $\pm 1^\circ\text{C}$  uniform temperature zone of 15 cm. The chamber was evacuated and backfilled with argon gas to provide a protective atmosphere and then heated up to the test temperature.

The nominal hoop stress of the specimen,  $\sigma_n$ , was calculated from the equation

$$\sigma_n = \frac{R_o^2 + R_i^2}{R_o^2 - R_i^2} \times P,$$

where  $P$  was the specimen internal pressure at test temperature,  $R_o$  and  $R_i$  were the OD and ID of the specimen, respectively. The value of  $P$  was calculated from the Beattie-Bridgeman's equation of state of real gas.<sup>12)</sup> The time-to-failure was determined by pressure difference due to release of the internal gas of the specimen at failure in the chamber. The amount of crystal iodine was weighed and loaded into the glass ampoule. Before the specimen was connected to the pressurization system, the the

ampoule was provided into the inside of the specimen. Iodine concentration was defined as the amount of loaded iodine divided by the total surface area of the specimen. Because very small amount of iodine was difficult to handle, it was not possible to perform tests in the low concentration range.

To examine the SEM fractographs, the failure section was broken open in the liquid nitrogen by bending the half ring which was cut from the failed specimen.

### 3. Results and Discussion

#### 3.1. The effects of iodine concentration

Fig. 3 shows the variation of time-to-failure of the specimen with iodine concentration at the fixed temperature of 603°K and the hoop stress of 467 MPa. The time-to-failure sharply decreases with the concentration up to 0.2 mg/cm<sup>2</sup>, but above this value it is almost constant. Failure type, macroscopically, changes from split to pinhole as the concentration increases. This indicates that there is the critical value of iodine concentration for SCC, which has been generally defined as a concentration at half point of the difference between time-to-failures or failure strains. The value is about 0.2 mg/cm<sup>2</sup>. These behaviors are consistent with other studies.<sup>7,8)</sup>

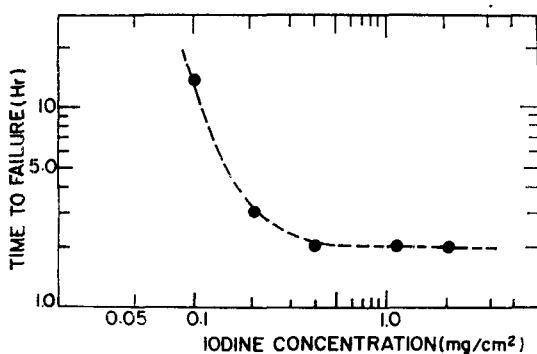


Fig. 3. Time-to-failure as a Function of Iodine Concentration at 603°K and 467 MPa.

Cubiccioni et al.<sup>13)</sup> reported that iodine was transferred as gaseous ZrI<sub>4</sub> or by surface diffusion into the crack where iodine became chemisorbed on the fresh metal surfaces and only a small pressure of monatomic iodine remained in the gas. By Shann et al.,<sup>14)</sup> the time-to-failure varied inversely with the equivalent iodine pressure and the activation energy for I-SCC was about 7 Kcal/mol, which suggested that the rate-controlling step was associated with gaseous diffusion or perhaps surface diffusion process. In this study, moreover, there is a critical concentration and above this value the time-to-failure is almost independent of the concentration, which is indicative of a surface diffusion process. Considering these results, it can be summarized that iodine is transferred by surface diffusion into the crack rather than as gaseous ZrI<sub>4</sub>.

#### 3.2. The Effects of Stress

The stress dependence of the time-to-failure at 633°K and 0.8 mgI<sub>2</sub>/cm<sup>2</sup> was shown in fig. 4. The specimens tested without iodine fail in a stress-rupture mode and slightly dependent on stress. The fracture surface shows the ductile-dimple features. In tests with iodine, the time-to-failure vs. stress curve falls largely below the curve representing the stress-rupture tests without iodine, but it appears to flatten

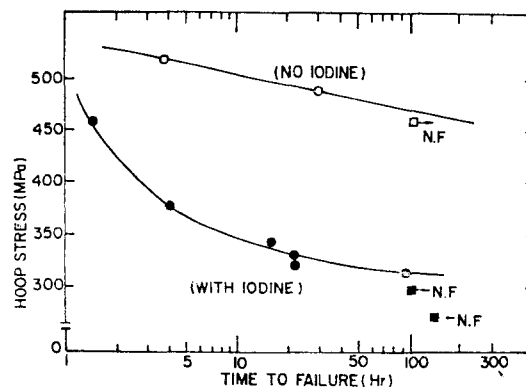


Fig. 4. Time-to-failure as a Function of Hoop Stress at 633°K and 0.8mgI<sub>2</sub>/cm<sup>2</sup>.

out near the stress of about 310 MPa. This threshold stress of 310 MPa is consistent with the values determined by other studies<sup>3,6)</sup> for similar material, but is much higher than that for the irradiated Zircaloy-4. The curve, generally, appears to flatten out at low stress but not completely. Thus, the threshold stress should be defined as the stress which corresponds to a finite time-to-failure. Because the stresses at 20 and 100 hrs are almost the same, it is reasonable even if the threshold stress is determined as the stress at about 20 hrs. The specimens with iodine exhibit the pinhole type failure and cleavage feature at stresses below about 380 MPa, but the specimens at higher stresses show the split type failure and have the cleavage and ductile-dimple mixed fracture surface.

In fig.5. SCC susceptibility at 603 °K and 0.8 mgI<sub>2</sub>/cm<sup>2</sup> is shown according to the tube suppliers. The SCC behaviors are similar, but the tube of supplier A is more resistant to SCC than supplier B. The threshold stress of supplier A is about 405 MPa and higher about 30 MPa than that of supplier B.

The specimens of both suppliers are the stress-relieved Zircaloy-4 cladding, As to supplier A, the mechanical properties of the specimens are UTS=610MPa, YS=480MPa, elonga-

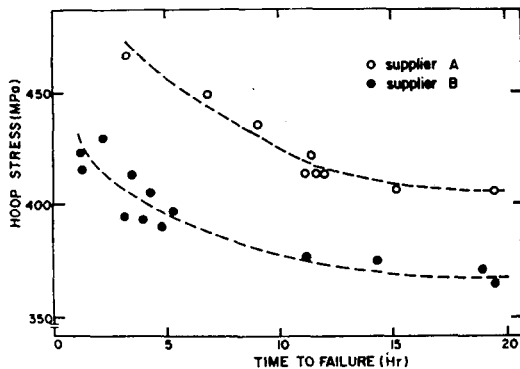


Fig. 5. The Influence of The Tube Supplier the I-SCC of Zircaloy-4 at 603°K and 0.8mgI<sub>2</sub>/cm<sup>2</sup>.

tion=27% in longitudinal tensile test and UHS (ultimate hoop stress)=830MPa, TCE (total circumferential elongation)=30% in burst test at room temperature and surface roughness=about 15 microinches. As to supplier B, UTS=618MPa, YS=485Mpa, elongation=35%, UHS=810MPa, TCE=23% and surface roughness=about 20 microinches. The significant difference in these properties is the toughness. The toughness of supplier A is worse in axial direction but better in circumferential than that of supplier B. Therefore, it is suggested that the threshold stress and susceptibility of I-SCC for the internal pressurization test are dependent on the toughness in circumferential direction but nearly independent of the toughness in axial direction.

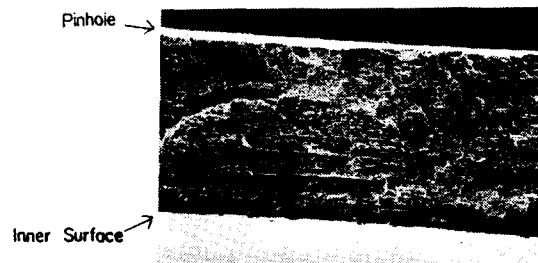


Fig. 6. Cross Section of the Typical Specimen Surface with Pinhole Failure. The Dotted Line Indicates the Boundary of SCC and Ductile Fracture Produced by Mechanical Bending.  $\times 75$

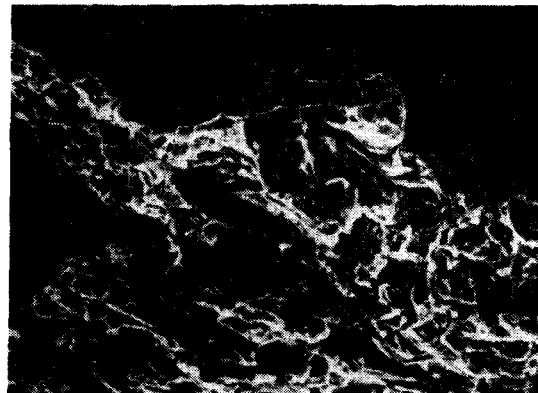


Fig. 7. Fracture Surface of The Specimen with Axial Crack.

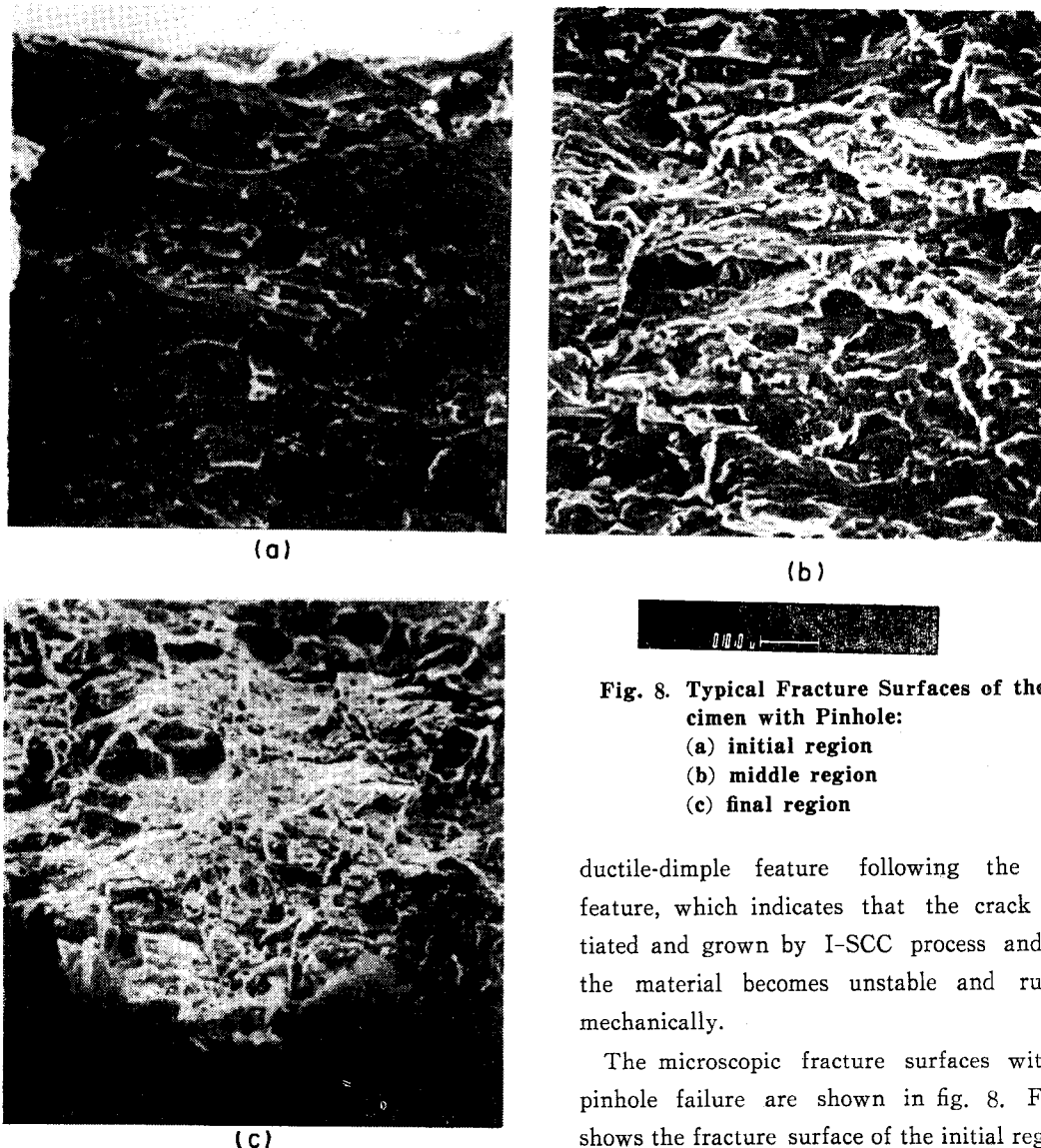


Fig. 8. Typical Fracture Surfaces of the Specimen with Pinhole:

- (a) initial region
- (b) middle region
- (c) final region

ductile-dimple feature following the brittle feature, which indicates that the crack is initiated and grown by I-SCC process and then the material becomes unstable and ruptures mechanically.

The microscopic fracture surfaces with the pinhole failure are shown in fig. 8. Fig. 8a shows the fracture surface of the initial region in I-SCC process, which is adjacent to the specimen inner surface. On the inner surface, there is the uniform oxide layer with 2 to 3  $\mu\text{m}$  thickness and this layer appears to be very brittle. Cracks seem to be formed beneath the layer and grown stepwise. Most of the fracture surface shows transgranular features with the river pattern and the wedge-shaped cracks between cleavage facets, but intergranular features are not almost observed. A cleavage facet appears to be extended in axial direction and narrowed in radial of the

### 3.3. Fractographic Study

There are two types of I-SCC i.e. the pinhole and the split crack. The typical macroscopic view of the pinhole fracture is given in fig. 6. The pinhole generally appears as a X-mark on the cladding outer surface, but as a long flaw which is composed of a few longitudinal slits with 1~2mm length on the inner surface. The entire fracture surface seems to be brittle. The typical fracture surface of the specimen with split failure is shown in fig. 7. It has the

tube specimen. Considering that a river pattern is generally consistent in a grain and that a grain of the specimen is expended axially, a cleavage facet seems to correspond to a grain. Striation and fluting features, which are the general character of brittle fracture in hcp materials,<sup>15)</sup> are not almost observed. It results from the high textural structure specimen and the little ductile-tearing process due to relatively low stress and strong chemical attack in the initial stage.

Fig. 8b shows the fracture surface of the middle region in I-SCC. Cleavage and ductile-tearing mixed features are shown. Cleavage facets with the river pattern, which indicates the direction of microscopic crack propagation in that portion, are often separated by tearing regions. It is, however, observed that cracks propagated stepwise.

The final stage of failure is shown in fig. 8c, which part is adjacent to the specimen outer surface and is fractured by the featureless mechanical fracture rather than the stepped cleavage fracture.

In polycrystalline materials the cleavage plane in a grain is not consistent with that in the neighbouring grains. Once, thus, a cleavage crack proceeds along the cleavage plane in a grain, it is believed that the crack should stop at grainboundary until the next cleavage crack nucleates. During this interval time, iodine may diffuse into and weaken the grainboundaries near the crack tip and then cause the w-shaped cracks.<sup>16)</sup> If the interval time is long, the w-shaped cracks will penetrate and consequently, the intergranular cracks will appear. Otherwise, a crack will proceed along a cleavage plane again. Therefore, it is thought that the cracks should propagate from one grain to others stepwise and that the ratio of transgranular to intergranular feature in the fracture surface should vary with the characters of the cladding material and the test conditions.

As the crack proceeds, the stress at its tip increases due to the stress concentration and/or reduction of the net cross section of the specimen, but the amount of iodine at the tip may decrease. During the interval time, then, the ductile-tearing fracture rather than nucleation of the cleavage crack should occur readily. Therefore, the transgranular and ductile-tearing mixed fracture seems to be observed in the intermediate stage in I-SCC.

In the final stage, the material is mechanically unstable and fractures in ductile mode rather than in brittle mode.

For the specimen with an axial crack, the fracture surface shows the ductile-dimple feature following the brittle feature rather than the only ductile feature. It is supposed that once the stress at the crack tip which proceeded by I-SCC reaches a certain value and overcomes the constraint of the intact material around the crack tip, the material should be stress-ruptured and show the ductile feature with dimples. It cannot be excluded, however, that the brittle and the ductile-dimple fracture occur simultaneously.

#### 4. Conclusions

(1) There is a critical iodine concentration for I-SCC of about  $0.2 \text{ mg/cm}^2$  at  $603^\circ\text{K}$ . Iodine seems to be transferred by surface diffusion into crack tip rather than as gaseous  $\text{ZrI}_4$ .

(2) There is a threshold stress for I-SCC and the value varies with the test temperature and the mechanical properties of the specimen.

(3) The fracture surface shows that the cracks should propagate stepwise from one grain to others until the material is unstable and then ruptured mechanically. The initial region consists of transgranular features and wedge-shaped cracks. As the crack proceeds, the transgranular and ductile-tearing mixed feature appears.

### Acknowledgment

The authors thank S.J. Park for consistent operation in the work and NFFD members in KAERI for assistance in preparation and machining of the specimen. They also gratefully acknowledge D.S.Shon and S.Kim for directing the experimental apparatus.

### References

1. H.S. Rosenbaum, *Electrochem. Tech.*, **4**, 153 (1966).
2. B. Cox and J.C. Wood, "proc. conf. of the Corrosion Division of the Electrochemical soc.", Corrosion Problems in Energy Conversion and Generation, 275 (1974).
3. D. Cubicciotti and R.L. Jones, EPRI NP-717 (1978).
4. F.L. Yaggee, R.F. Mattas and L.A. Neimark, EPRI NP-1155 (1979).
5. J.C. Wood, *J. Nucl. Mat.*, **45**, 105 (1972~3).
6. D. Cubicciotti et al., EPRI NP-1329 (1980).
7. M. Peehs et al., "Zirconium in the Nuclear Industry; 4-th conf.", ASTM STP-681, 244 (1979).
8. P. Hofman and J. Spino, *J. Nucl. Mat.*, **107**, 297 (1982).
9. K. Videm and L. Lunde, "ENS and ANS conf. on Fuel Element Failures caused by I-SCC", Paris (1975).
10. K. Pettersson and W. Stany, "5-th International conf. on Zirconium in the Nuclear Industry", B-1, Boston (1980).
11. S. Shimada and M. Nagai, *J. Nucl. mat.*, **114**, 222 (1983).
12. J.S. Shieh, "Principles of Thermodynamics", McGraw-Hill Kogakusha, Japan (1975).
13. D. Cubicciotti, R.L. Jones and B.C. Syrett, "Zirconium in the Nuclear Industry; 5-th Conf.", ASTM STP-754, 146 (1982).
14. S.H. Shann and D.R. Olander, *J. Nucl. Mat.*, **113**, 234 (1983).
15. I. Aitchison and B. Cox, *Corrosion*, **28**, 83 (1972).
16. G.E. Dieter, "Mechanical Metallurgy", 2nd ed., McGRAW-HILL, (1976).